JOURNAL OF GEOPHYSICAL RESEARCH, VOL. 113, C06022, doi:10.1029/2006JC004079, 2008

Response of the global ocean to Greenland and Antarctic ice melting

D. Stammer[1,2]

Received 28 December 2006; revised 8 December 2007; accepted 18 March 2008; published 24 June 2008.

[1] We investigate the transient response of the global ocean circulation to enhanced freshwater forcing associated with melting of the Greenland and Antarctic ice sheets. Increased freshwater runoff from Greenland results in a basin-wide response of the North Atlantic on timescales of a few years, communicated via boundary waves, equatorial Kelvin waves, and westward propagating Rossby waves. In addition, modified air-sea interaction plays a fundamental role in setting up the basin-scale response of the Atlantic circulation in its subpolar and subtropical gyres. In particular, the modified ocean dynamics and thermodynamics lead to a depression in the central North and South Atlantic that would not be expected from linear wave dynamics. Moreover, the heat content increases on basin and global scales in response to anomalous freshwater forcing from Greenland, suggesting that the ocean's response to enhanced freshwater forcing would be a coupled problem. Other parts of the world ocean experience a much slower adjustment in response to Greenland freshwater forcing, communicated via planetary waves, but also involving advective/diffusive processes, especially in the Southern Ocean. Over the 50 years considered here, most of the sea level increase associated with freshwater input from Greenland remains in the Atlantic Ocean. In contrast, ice melting around Antarctica has a much reduced effect on the global ocean. In both cases, none of the basins came to a stationary state during the 50-year experiment.

Citation: Stammer, D. (2008), Response of the global ocean to Greenland and Antarctic ice melting, *J. Geophys. Res.*, *113*, C06022, doi:10.1029/2006JC004079.

1. Introduction

[2] The focus of this paper is the response of the regional and global ocean to localized freshwater forcing originating from enhanced melting of polar continental ice sheets. The study was stimulated by recent suggestions that parts of the Greenland and Antarctic ice masses are experiencing an accelerated mass loss and by speculations that over the next century further increased amounts of freshwater may leave both ice sheets in the form of melt water runoff. Regional and global sea level will respond to this extra freshwater input. However, the details of this adjustment process are unknown, but are expected to be far from trivial. In particular, an often assumed instantaneous increase in global sea surface height (SSH) seems unlikely, given what we know already about ocean dynamics.

[3] Recent estimates indicate that between 1996 and 2004 Greenland has lost 50 to 100 Gt net freshwater per year [*Thomasi et al.*, 2006; *Velicogna and Wahr*, 2005]. *Rignot and Kanagaratnam* [2006] suggest that the net Greenland melting rate has accelerated to about 200 Gt/a in 2005; moreover, *Zwally et al.* [2005] estimated that an equivalent net mass loss takes place over the Antarctic ice shield as well. Averaged over the last 50 years, about 0.5 mm/a increase in global SSH was estimated to have originated from glacial melting [*Dyurgerov and Meier*, 2005], but this number is close to 1 mm/a now [*Nerem et al.*, 2006]. If accelerating even further during the next century, the melt water originating from polar continental ice sheets could potentially lead to an increase in SSH that would exceed the global and regional SSH increase expected from a thermal expansion of the ocean [e.g., *Church et al.*, 2001].

[4] To understand in detail how the basin and global ocean circulation adjusts to enhanced local freshwater forcing, two different aspects are of interest. The first is the short-term effect of ice melting on regional sea level, i.e., the spreading and redistribution of the freshwater volume in the ocean after leaving continental ice sheets and the subsequent local and global adjustment of the dynamics and thermodynamics of the ocean state. The second is the long-term effect of freshwater forcing on dense water formation in the high-latitude North Atlantic and thereby on the strength of the meridional overturning circulation (MOC) and on an associated redistribution of heat and volume in the ocean. The latter problem was discussed extensively in recent years, for example, by *Broecker et al.* [1989] who suggested that dumping of continental freshwater reservoirs into the subpolar North

[1]Institut für Meereskunde, Universität Hamburg, Hamburg, Germany.
[2]Also at Scripps Institution of Oceanography, University of California, San Diego, La Jolla, California, USA.

0148-0227/08/2006JC004079$09.00

Atlantic in the past could have led to reduced formation of dense water in the North Atlantic and an associated reduction of the MOC.

[5] More recently, *Gerdes et al.* [2006] investigated the reaction of a global coupled ocean-sea ice model to an increase of fresh water input into the northern North Atlantic under different surface boundary conditions, ranging from simple restoring of surface salinity to the use of an energy balance model (EBM) for the atmosphere. Like other studies [e.g., *Landerer et al.*, 2007], their emphasis was on the long-term changes in salinity as well as the adjustment of the MOC.

[6] The subject of our study is complementary to the above investigations: Rather than thinking about the long-term reaction of the general circulation and the MOC to greenhouse gas forcing, we are primarily interested in the transient adjustment of the regional and global ocean circulation, on timescales up to a few decades, to freshwater forcing injected locally in the North Atlantic around the coast of Greenland or to the Southern Ocean around Antarctica. We are especially interested in processes involved in the early redistribution of the injected freshwater and in the respective adjustment of the density field and of sea level on regional, basin and global scale.

[7] Because of the potential for substantial mass loss from Greenland during future centuries and the implication of increasing sea level to the coastal world population (including that of islands), a detailed understanding of the near-term, transient reaction of the regional and global sea level to locally increased freshwater input into the subpolar oceans is urgently needed. Related is the question of separating out different processes and phenomena in existing altimetric observations of SSH, including those caused by melting of polar ice sheets. Knowing the time and space scales and the pattern of the expected ocean response could be essential for an early identification of the adjustment of the North Atlantic circulation in response to Greenland melting and distinguishing it from associated effects in geoid or rebound changes in altimeter data [*Mitrovica et al.*, 2001].

[8] Important questions that need to be addressed in this respect include the following.

[9] 1. What are the details of the basin-wide response of salinity, temperature and SSH during the first decades after the onset of increase melting polar ice caps?

[10] 2. What are the implications of this response for air-sea feedbacks?

[11] 3. How does the basin-wide response of the North Atlantic to freshwater forcing from Greenland compare to SSH adjustments in other basins and what are associated time and space scales?

[12] 4. How important is the exact location of the perturbation; that is, does Greenland ice melting lead to different changes in regional and global SSH adjustment as compared to melting in the southern hemisphere? Would both work in the same direction or partially cancel out?

[13] To address those questions we will first discuss in Section 2 the model set up and the experiments. In section 3 we will discuss the adjustment of the regional and global hydrography, sea level and transports to enhanced freshwater injected around Greenland. In section 4 we will contrast those results to ones obtained by perturbing the Southern Ocean. Concluding remarks will follow in section 5.

2. Model Setup

[14] Model results discussed in this paper are based on the MIT ocean general circulation model [*Marshall et al.*, 1997a, 1997b], which uses the primitive equations on a staggered "C-grid" [*Arakawa and Lamb*, 1977] under the Boussinesq approximation. Spatial coordinates are longitude, latitude, and height. For present purposes, we used a hydrostatic version with an implicit free surface, a full surface mixed layer model [*Large et al.*, 1994] and an eddy parameterization [*Gent and McWilliams*, 1990]. The model was configured globally with a 1° horizontal resolution over ±80° in latitude with 23 levels in the vertical. Laplacian viscosity and diffusivities are used, with $\nu_h = 1 \times 10^4$ m^2/s and $\kappa_h = 10^3$m^2/s and $\nu_v = 10^{-3}$ m^2/s and $\kappa_v = 10^{-5}$ m^2/s, in the horizontal and vertical, respectively, as well as a no-slip bottom, and free-slip lateral boundary conditions. Horizontal friction was scaled according to a $\cos^{\alpha}(\phi)$ power law, with ϕ being latitude, and $\alpha = 2.25$ to account for the decreasing distance between meridians toward the poles. Northern and southern boundaries were closed. The model topography was derived from the high-resolution topography data provided by *Smith and Sandwell* [1997] with 1/30° horizontal resolution. We note that the set-up of the control run is essentially similar to the one used for the global 1° global synthesis of ocean observations performed by the ECCO (Estimating the Circulation and Climate of the Ocean) consortium [*Stammer et al.*, 2002] which is described in detail by *Stammer et al.* [2004] and by *Köhl et al.* [2007]. We note that similar model setups have been used repeatedly in the past to study changes in SSH and ocean circulation during the last decades [e.g., *Wunsch and Heimbach*, 2006; *Wunsch et al.*, 2007; *Stammer et al.*, 2002; *Köhl et al.*, 2007].

[15] The model was initialized in 1948 from the *Levitus et al.* [1998] January temperature and salinity climatology and was run over a 50-year-long period. During this period the model was driven by daily net heat and freshwater forcing obtained from the National Center for Environmental Prediction/National Center for Atmospheric Research (NCEP/NCAR) reanalysis (RA1) [*Kalnay et al.*, 1996]. Wind stress fields were provided twice per day. Similar to most of the above model studies, net freshwater fluxes, *FW*, were converted into virtual salt fluxes, $F_s = FW * S_0$, using a reference salinity of $S_0 = 35$ psu (see *Prange and Gerdes* [2005] for a discussion of the adequacy of this formulation for present purposes). In addition to the surface forcing, the surface temperature and salinity fields were relaxed toward monthly Reynolds temperature fields [*Reynolds et al.*, 2002] (NOAA Optimum Interpolation (OI) SST V2 data provided by the NOAA-CIRES Climate Diagnostics Center, Boulder, Colorado, USA, from their web site at http://www.cdc.noaa.gov/) and toward the Levitus monthly salinity climatology [*Levitus et al.*, 1998] (both with a 30-day relaxation timescale) as is required if one forces a model with center-provided surface buoyancy forcing. This is equivalent to driving the model with Bulk formula based on the NCEP/NCAR atmospheric state and the actual model SST, as discussed in detail by *Garnier et al.* [2000]. Important for

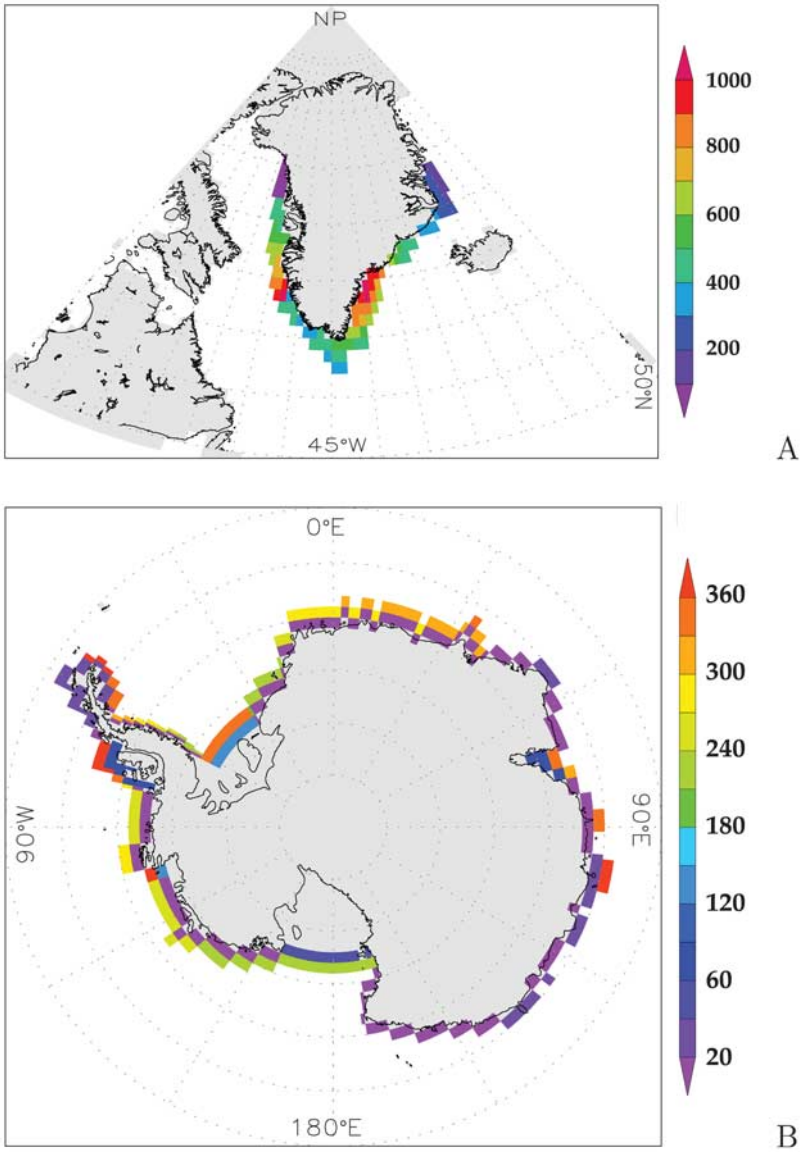

Figure 1. Surface freshwater flux anomalies (in m^3/s) per model grid point associated with the mass loss of polar ice sheets and added to the NECEP/NCAR net freshwater forcing after division by the surface area of each grid cell for (a) the Greenland run and (b) the Antarctic run.

the interpretation of later results is that this formulation does imply a feedback of the perturbed ocean to the unperturbed atmosphere, an assumption that seems realistic as long as perturbations in the ocean are small (but see discussion below).

[16] Our experiment consists of a control run and two subsequent runs in which the freshwater forcing was perturbed locally in two separate regions, one centered around Greenland, one localized around Antarctica. To investigate the response of the ocean to increased freshwater input, we will use as a signal the differences between the perturbed runs minus the initial reference run. The following analysis will be based on monthly mean difference fields of temperature, T, salinity, S, the horizontal flow field, $\mathbf{v}$, and of sea surface height, SSH.

[17] In a first perturbation run, a freshwater anomaly was added permanently (over the 50-year period) to the NCEP/NCAR surface net freshwater forcing off Greenland, mimicking an enhanced runoff of Greenland melt water. In a second run a respective freshwater perturbation was added to the NCEP surface freshwater forcing fields to simulate the effect of melting over Antarctica. In both cases the construction of respective anomalies in the surface forcing was oriented along observations of mass loss from Greenland or Antarctica, as they are provided, for example, by *Krabill et al.* [2004] and *Jacobs et al.* [1992, 1996].

[18] To construct an anomaly in surface freshwater forcing from information about ice mass loss, the loss of ice mass has to be first converted into a volume flux of

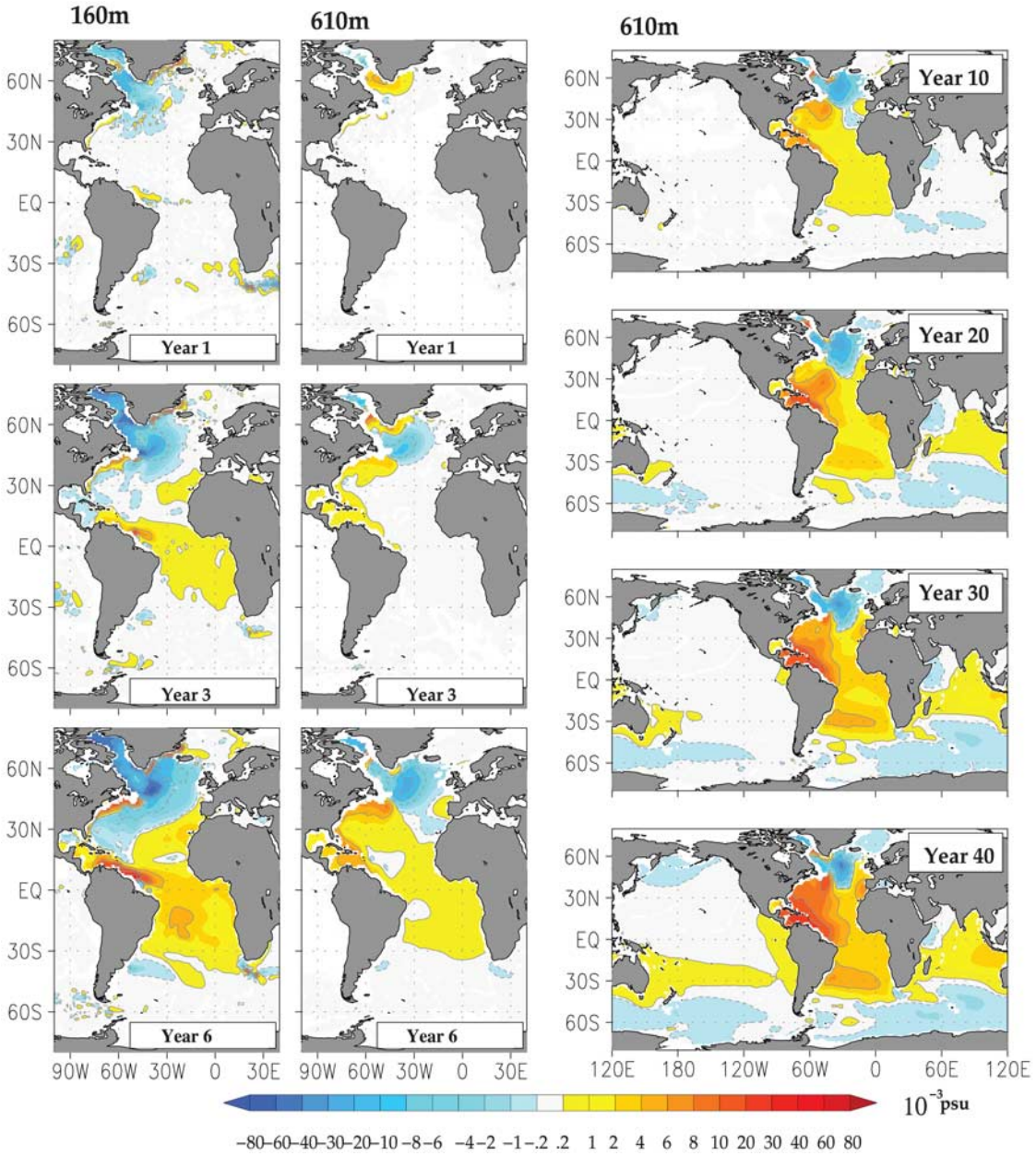

Figure 2. (two left columns) December-mean salt anomalies at 160 m and 610 m depth from the model years 1, 3, and 6 of the Greenland run. (right) December-mean salt anomalies at 610 m depth are shown from the years 10, 20, 30, and 40.

freshwater and spread over the coastal regions. This is common, for example, in preparing runoff data sets and is described in detail by B. M. Fekete et al. (An improved global spatially distributed runoff data set based on observed river discharge and simulated water balance, unpublished report, 1999). Figure 1a shows the associated surface volume flux perturbation (in m^3/s) for each grid cell of the model. A respective plot resulting from Antarctica is shown in Figure 1b. The fields shown were converted to surface freshwater flux anomalies (in m/s) by normalizing them with the surface area of each grid cell and the respective field was added to NCEP net freshwater flux anomalies. (see also Figure 3 of *Gerdes et al.* [2006] for a construction of a similar surface freshwater flux anomaly field).

3. Results From Greenland Ice Melting

3.1. Salinity and Temperature Response

[19] The response of the model's salinity field to increased Greenland freshwater forcing can be illustrated in terms of a temporal sequence of December mean salinity anomalies, S', plotted in Figure 2 from different depth levels. A negative salinity anomaly, appearing at 160 m depth and above south of Greenland in year 1, spreads eastward during the following years. At the same time,

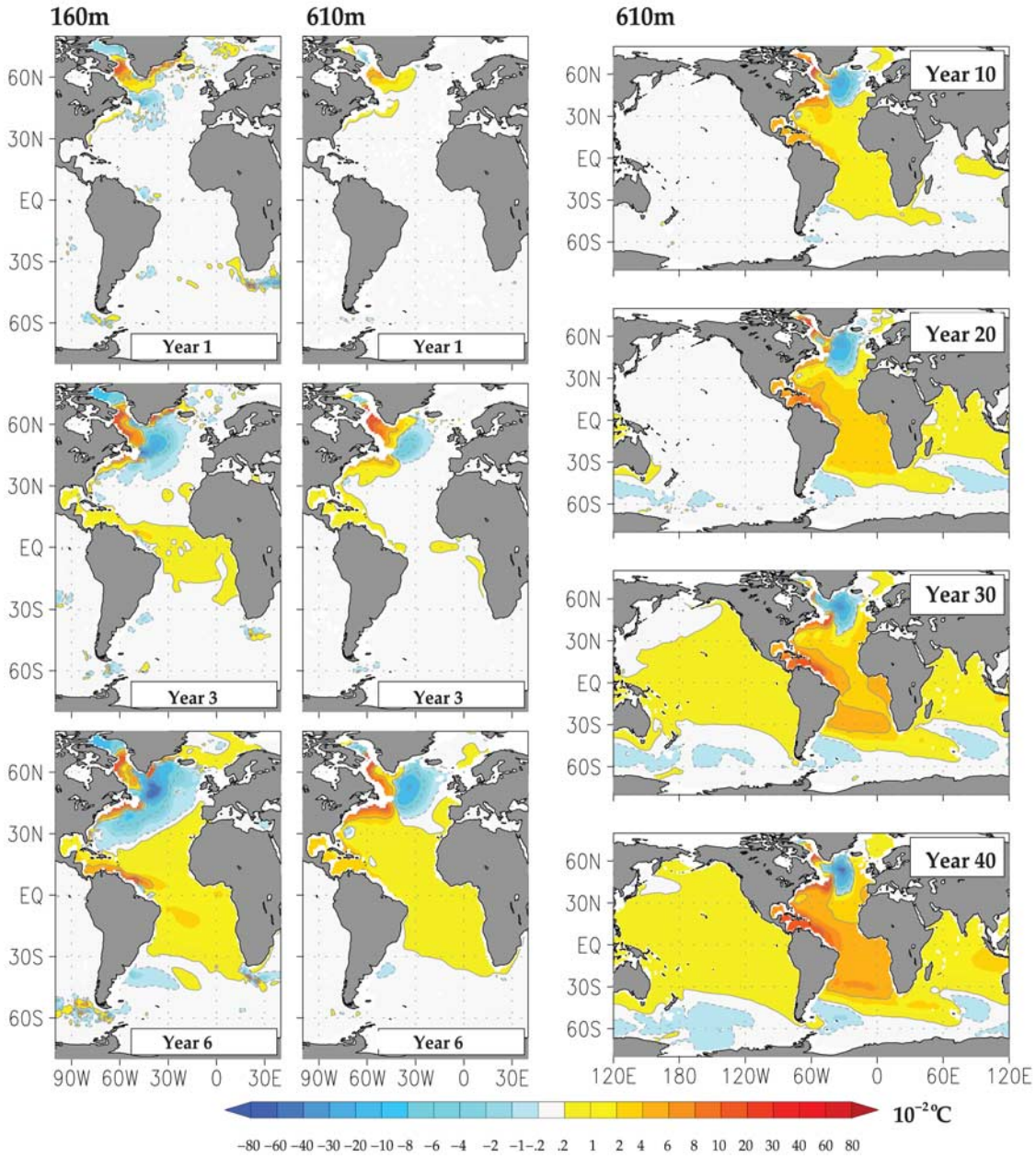

Figure 3. (two left columns) December-mean potential temperature anomalies at 160 m and 610 m depth from the model years 1, 3, and 6 of the Greenland run. (right) December-mean salt anomalies at 610 m depth are shown from the years 10, 20, 30, and 40.

positive values of S', appearing south of Flemish Cap, spread equatorward along the western boundary and reach from there into the eastern part of the Atlantic, before they propagate poleward in both hemispheres along the eastern coastline of the Atlantic. During year 5, negative salinity anomalies cover most of the subpolar North Atlantic and also reach southward to the Antilles west of the Mid-Atlantic Ridge. The remaining part of the Atlantic shows positive S' values.

[20] Going deeper to the 600 m depth level, the situation reverses in that initial salt anomalies are positive around Greenland in year 1 owing to reduced convection and an associated reduction in downward transport of fresher surface waters. Respective positive salinity anomalies spread southward along the western continental shelf and, in year 3, reach over to the eastern side of the basin along the equator. A negative salt anomaly appears east of Flemish Cap underneath a positive near-surface salt anomaly 2–3 years after the onset of the perturbation in the surface freshwater forcing. Both are being advected eastward by the background flow field.

[21] Because the addition of freshwater around Greenland and its subsequent spreading across the subpolar basin adds stability to the upper ocean and thereby reduces convection, the temperature field of the basin responds significantly to the anomalous Greenland freshwater forcing Figure 3. The respective temperature response involves positive subsurface temperature anomalies emerging initially along the

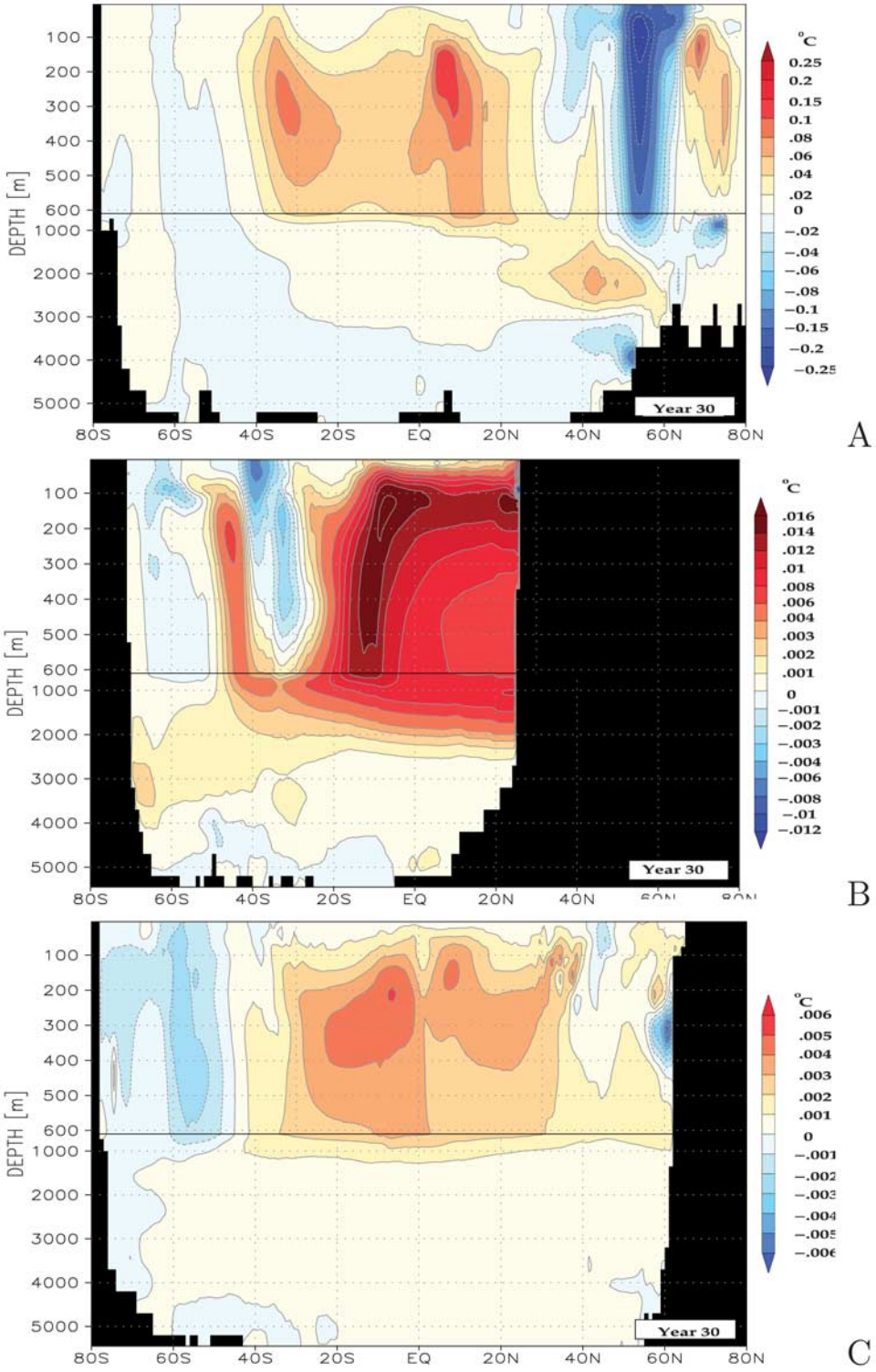

Figure 4. Meridional sections of potential temperature anomalies from year 30, plotted along (a) 30°W in the Atlantic Ocean, (b) 80°E in the Indian Ocean, and (c) 180°E in the Pacific Ocean as a function of depth.

coast of Greenland. They spread equatorward subsequently and reach over into the eastern basin along the equator and the poleward along the eastern coast of the Atlantic in both hemispheres. The positive subsurface temperature anomalies off Greenland, which result from the increased stratification and the associated reduced convection, lead to near-surface layers of the subpolar North Atlantic that are much cooler than normal. Once those cooler surface temperature anomalies reach into the North Atlantic Current, they trigger convection east of Flemish Cap, causing the deeper layers to

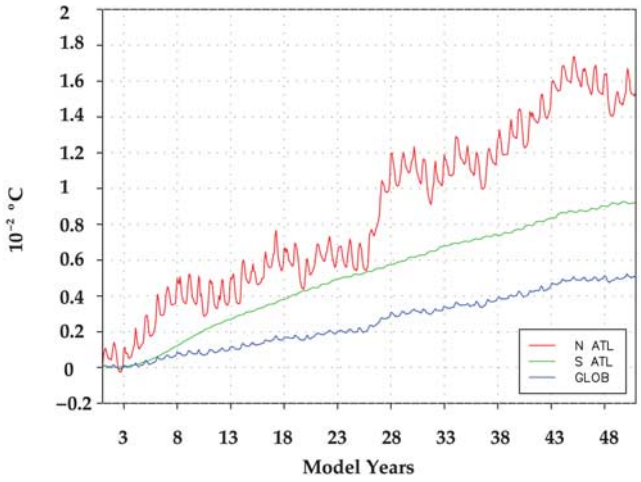

Figure 5. Basin-integrated potential temperature anomalies computed separately for the North Atlantic (red), the South Atlantic (green), and globally (blue).

cool more than normal. At the same time, this convection leads to negative salt anomaly observed at 610 m depth in Figure 2.

[22] Findings from Figures 2 and 3 can be summarized as follows.

[23] 1. Adding freshwater to the area around the Greenland coast (imposed in the model through negative surface salt fluxes) leads to fresher than normal surface water there. The anomalously fresh water initially stays in the surface layers and is advected by the East Greenland current and its extension into and around the Labrador Sea.

[24] 2. After reaching the southern tip of the Labrador Sea, the fresher than normal water is advected into the subpolar gyre of the North Atlantic. As a result, much of the subpolar gyre is anomalously fresh after about 3 years.

[25] 3. Fresh surface waters in the Labrador Sea lead to reduced convection there. As a result, the near-surface water gets anomalously cold (through surface cooling), while subsurface waters stay unusually warm (owing to reduced convection). A respective warm anomaly can be found at 160 to 630 m depth, and appears to propagate from the Labrador Sea equatorward along the western coast. The warm anomaly reaches the tropical Atlantic in less than 3 years, crosses into the eastern tropical Atlantic via a Kelvin wave and from there starts to fill the eastern basin.

[26] 4. Along with reduced convection and warmer than normal water, a salty subsurface anomaly also appears, created by the reduced interaction of subsurface waters with surface waters. This salty anomaly travels along with the warm anomaly down the coast and starts to fill the low-latitude Atlantic and then the eastern Atlantic with anomalously salty water.

[27] 5. Surface waters become increasingly cold (owing to reduced convection) on their way around the Labrador Sea. Come Flemish Cap, the water has reached a temperature where it starts to trigger convection against the freshwater-induced stabilization, bringing anomalously fresh and cold water subsurface down to 630 m (and deeper). This anomaly is advected with the subpolar gyre northward, leading to a cold, denser, center of the subpolar gyre.

[28] 6. The density gradient in the Gulf Stream region resulting from the first adjustment is such that the Gulf Stream is slowed down, starting to carry less heat and salt northward. As a result, the western subtropical gyre becomes even cooler and fresher. This is equivalent to an anomalous southward current carrying the salt and temperature anomaly, created in the subpolar North Atlantic, southward.

[29] This latter concept is consistent with work by *Bryan* [1996], who showed that associated with anomalous heat input into the ocean due to CO_2 increase in the high-latitude zone, there is a relatively uniform sea level rise in low latitudes in both hemispheres due to the redistribution of heat by the anomalous MOC.

[30] During the first years, most anomalies in temperature and salinity are confined to the Atlantic. However, in year 10 the first anomalies reach into the Indian Ocean from where they evaded the tropical Pacific, filling the entire Pacific again in a Kelvin/Rossby wave fashion as it happened before in the Atlantic and as is characteristic for a global adjustment problem [*Cessi et al.*, 2004]. After 40 years, anomalies enter the Atlantic again via Drake Passage.

[31] To demonstrate the vertical extent of the models reaction to the freshwater perturbation around Greenland, Figure 4 shows vertical sections of potential temperature anomalies, crossing the Atlantic along 30°W, the Indian Ocean along 80°E and the Pacific along 180°E, respectively, and taking 30 years after the onset of the freshwater forcing. Overall, the magnitude of the temperature anomalies decreases from the North Atlantic to the Indian Ocean, to the Pacific. Nevertheless, a response in the subsurface temperature can be identified even in the latter basin, demonstrating the potential warming of the tropical and subtropical Indian Ocean and Pacific in response to the enhanced Greenland ice sheet melting.

[32] The degree to which the heat content of all individual basins is changing through the freshwater forcing of the subpolar North Atlantic is illustrated in Figure 5, showing time series of the anomalous temperature content, $\langle T' \rangle$, computed separately for the North Atlantic, the South Atlantic, and for the entire model domain. Unintuitively, the heat content of all basins increases through the entire 50-year run owing to enhanced freshwater forcing near Greenland, including the North Atlantic. This is caused by the anomalous surface temperatures, generated through changes in convection and circulation pattern, which are being relaxed back to the Levitus climatological monthly mean temperature fields. Anomalous ocean temperatures are expected to be damped by the unperturbed atmosphere and these interactions/feedbacks could therefore be realistic in nature (as long as they are relatively small).

3.2. SSH and Velocity Anomalies From Greenland Experiment

[33] A compact description of the model's dynamic response to freshwater forcing can be provided in terms of the time-evolution of SSH anomaly (Figure 6). The figure clearly resembles the adjustment of the global ocean to anomalous forcing in terms of Kelvin and Rossby waves, which was already visible in the temperature and salinity fields and which was discussed previously, for example, by *Bryan* [1996], *Hsieh and Bryan* [1996], *Huang et al.*

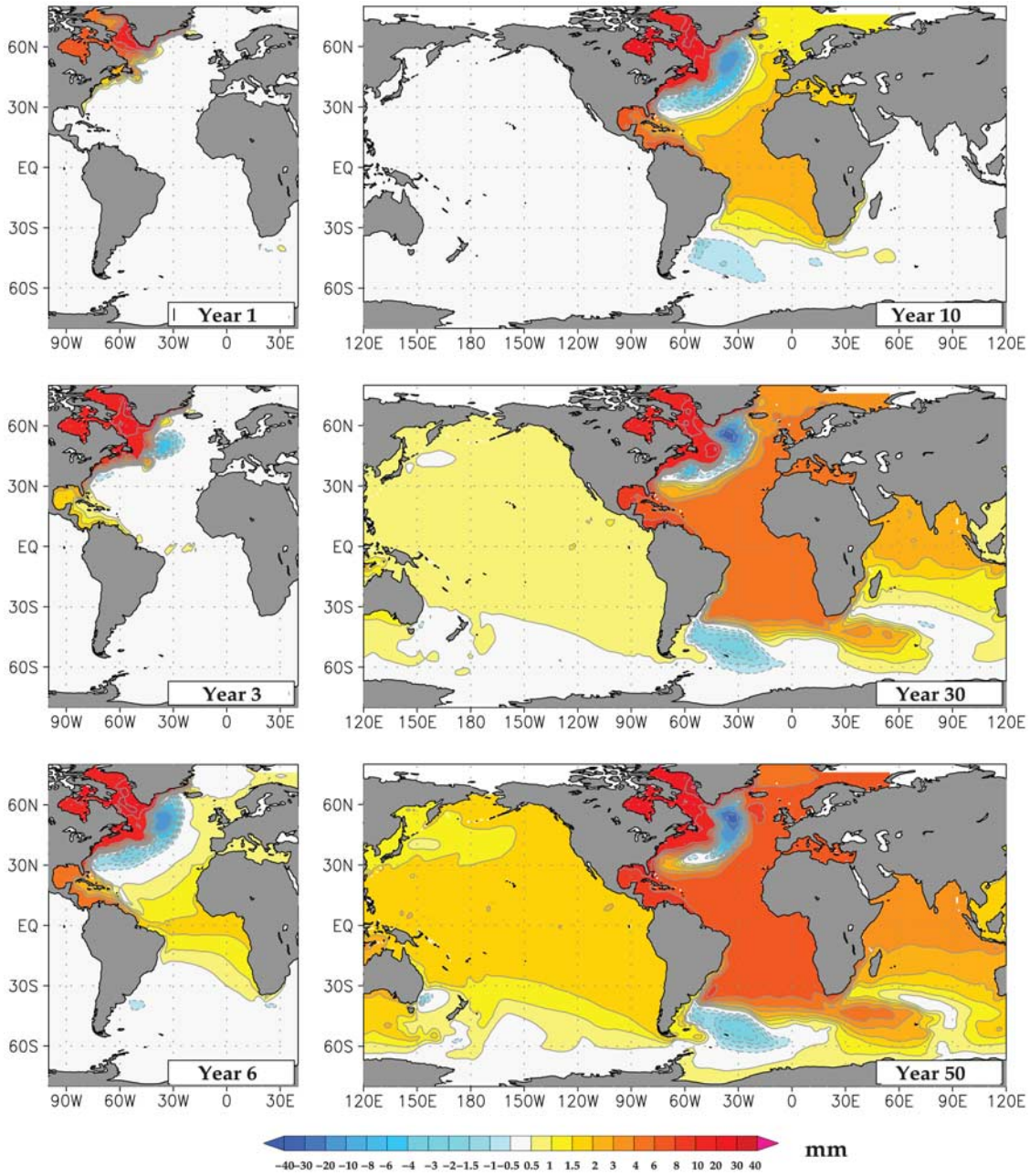

Figure 6. December-mean anomalies of SSH as they result from enhanced Greenland freshwater forcing. (left) SSH anomalies for the Atlantic from the years 1, 3, and 6. (right) Similar fields, but globally and for the years 10, 30, and 50.

[2000], *Goodman* [2001], *Cessi and Otheguy* [2003], and more recently by *Cessi et al.* [2004]. With respect to our specific application of freshwater forcing off Greenland, this adjustment starts with an initial boundary wave, propagating southward from the Labrador Sea toward the equator, where it crosses the Atlantic toward the eastern side. It subsequently propagates poleward in both hemispheres. The associated positive SSH anomaly located now along the east coast of the Atlantic radiates off baroclinic Rossby waves that, by moving westward, fill the basin with warm, elevated SSH anomalies from the east coast. After reaching the southern tip of Africa, the southern boundary wave crosses over into the Indian Ocean around Good Hope. After about 10 years, the positive, warm, SSH anomaly, associated with the freshwater forcing off Greenland in the subpolar North Atlantic, starts to raise SSH of the Indian Ocean and after 30 years has covered much of the Pacific Ocean.

[34] A comparison with previous results [cf. *Cessi et al.*, 2004] indicates that much of the large-scale response found here from Greenland freshwater forcing seems consistent with reduced-gravity planetary wave dynamics. However, there are some distinct differences from those earlier results, pointing toward a more complicated dynamical adjustment in our experiment based on primitive-equation dynamics which involve advective processes as well as air-sea interaction. Most conspicuously, we find a cold SSH depression

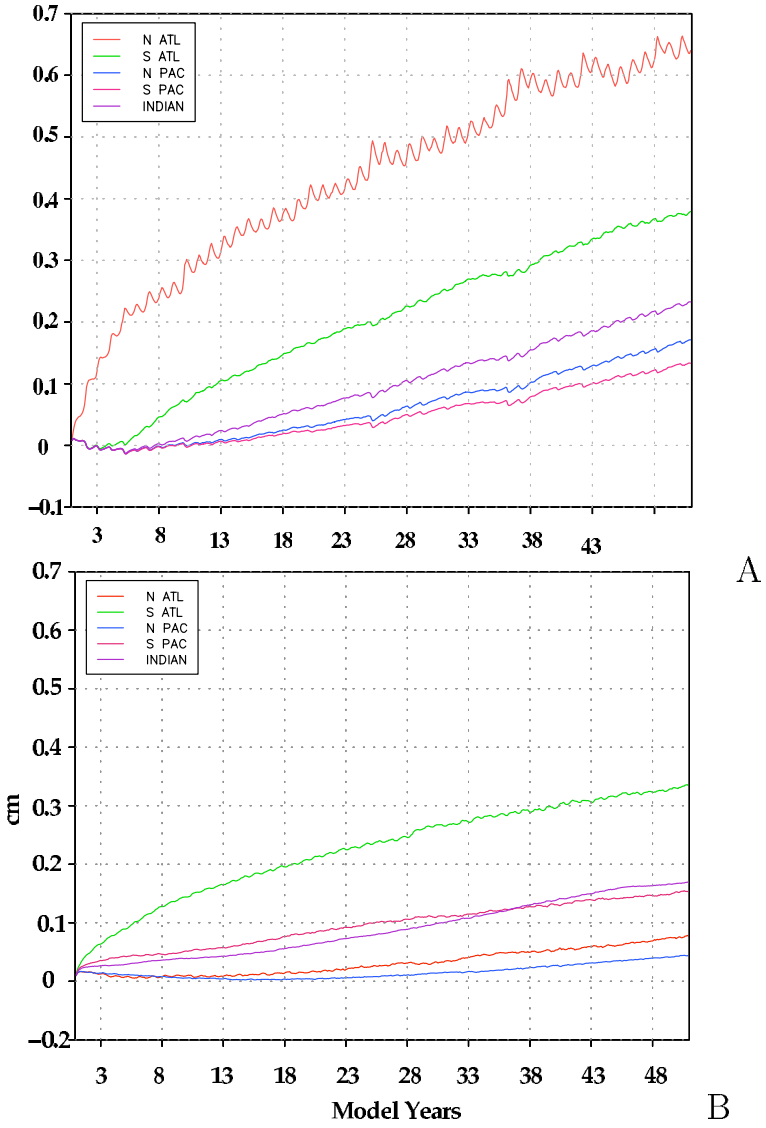

Figure 7. (a) Basin-integrated SSH anomalies resulting from the Greenland run, computed separately for the North Atlantic (red), the South Atlantic (green), the Indian Ocean (purple), and the North and South Pacific (blue and red, respectively). (b) Basin-integrated SSH anomalies resulting from the Antarctic run, computed separately for the North Atlantic (red), the South Atlantic (green), the Indian Ocean (purple), and the North and South Pacific (blue and red, respectively).

in the center of the subpolar North Atlantic which, after 5–8 years, also covers much of the western subtropical North Atlantic (Figure 3). This depression is associated with cold water mass anomalies and leads to spin-up of the subpolar gyre by about 1 cm/s; at the same time it slows down the subtropical gyre by about 0.5 cm/s. A similar depression appears after year 6 in the vicinity of the Malvinas confluence region and spreads eastward from there, thereby building an almost symmetric pattern of the South Atlantic SSH to what can be seen in the North Atlantic during year 50. Associated with those changes in SSH in the South Atlantic are changes in temperature and salinity that appear first near the surface and subsequently reach to deeper levels, much like what is found in the North Atlantic. Shortly before year 30, similar SSH patterns appear all along the entire southern ocean, suggesting that modified air-sea fluxes are again responsible for modifying the gyre circulation and thus SSH in the Southern Ocean, much like what happens in the North Atlantic.

[35] The timescale by which the SSH adjusts in individual basins to the Greenland freshwater forcing (Figure 7) is in stark contrast to results from *Huang et al.* [2000] who showed in their three-dimensional reduced-gravity ocean model that it takes many decades for changes in SSH forced in the North Atlantic to reach the Southern Ocean, which was not adjusted by the end of their 140 years calculation. The North Atlantic increases steadily in its basin-averaged height, reaching up to 0.7 cm at the end of the 50-year period. The South Atlantic remains constant until about year 5, when it also starts to rise simultaneously with the

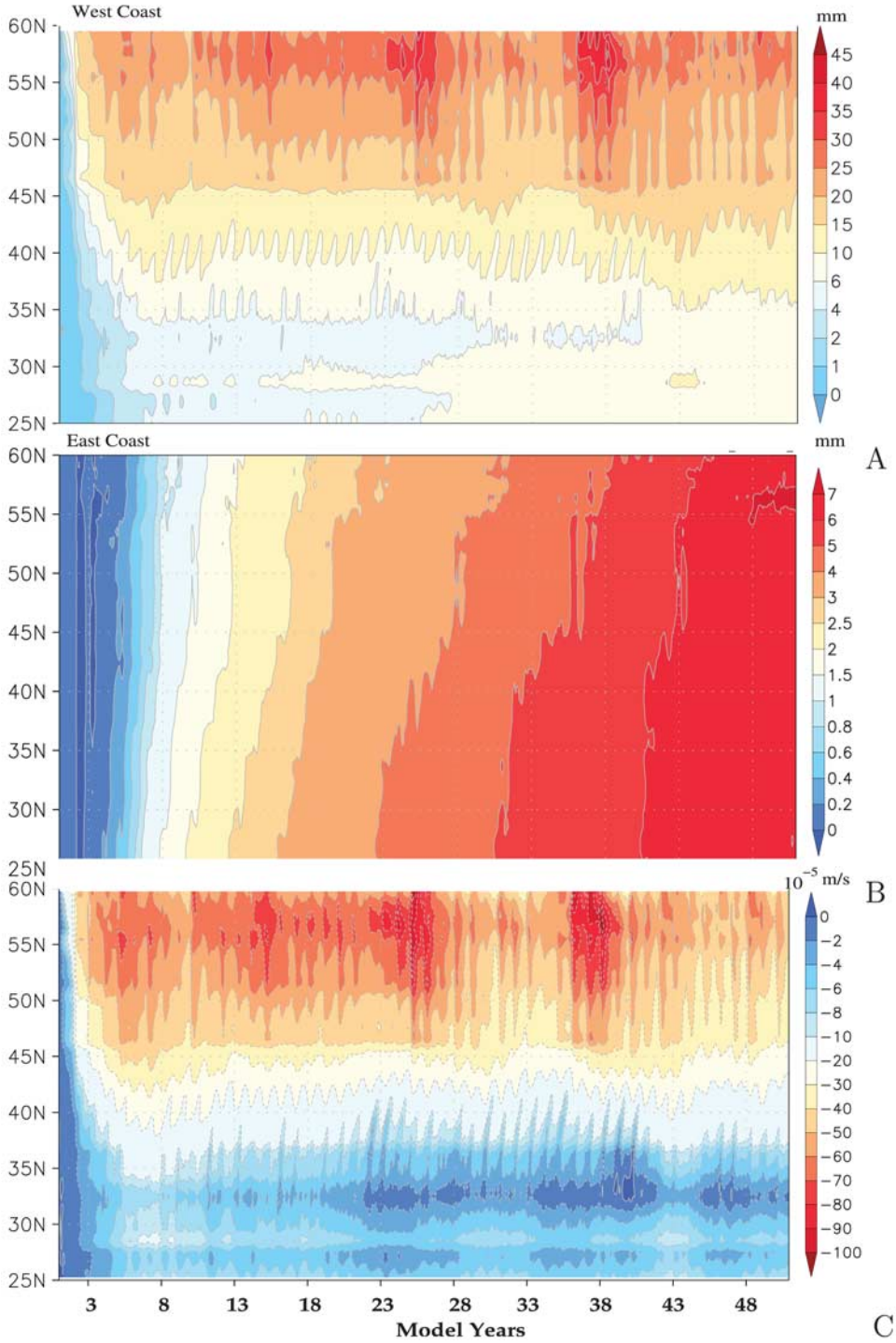

Figure 8. Time-latitude plots of SSH anomalies (a) along the west coast and (b) along the east coast of the North Atlantic. (c) Related basin-averaged meridional geostrophic velocity anomalies computed according to equation (1).

increase in heat content (Figure 5), followed by the Indian Ocean and the Pacific. Consistent with *Huang et al.* [2000], however, in Figure 7 the slowest increase in SSH occurs in the South Pacific. At the end of the 50-year run, the SSH adjustment has converged in none of the basins.

[36] The model has a free-surface formulation and can be used to study regional SSH changes. To correct the volume-conserving effect of the Boussinesq approximation on regional and global SSH, we followed the approach suggested by *Greatbatch* [1994], by assuring that the globally averaged bottom pressure remains constant over the entire model run. This assumption is equivalent to the model's mass remains unchanged.

[37] The transient SSH changes in the coastal North Atlantic are illustrated in Figure 8 showing SSH anomalies as they propagate along the west and east coasts of the North Atlantic, respectively. The initial positive SSH anomaly spreads quickly along the entire west coast, raising SSH at 25°N by 1 mm after 2 years and by about 1 cm after 50 years. The increase in higher latitudes is faster and at 55°N reaches about 3 cm after only 10–15 years. Consistent with Figure 6, it takes about 3 years before an increase in SSH can be observed at 25°N at the east coast, and then another 2 years until the anomaly reaches 60°N in the eastern North Atlantic. The subsequent increase in SSH along the east coast is steady, leading to about 0.7 cm at the end of the 50-year run. The associated propagation speed is slower than that of a pure Kelvin wave but agrees rather well with a boundary wave discussed in some detail by *Eden and Willebrand* [2001] (we note that according to *Hsieh et al.* [1983] the phase speed of a free Kelvin wave should not be reduced in our finite-difference numerical model formulated on a C-grid with current model parameters and resolution).

[38] Using the geostrophic relation, we computed the basin-averaged meridional velocity anomaly associated with the cross-basin gradients of SSH anomalies, $\Delta\,\eta(y)$, according to

$$\Delta v(y) = \frac{g}{f}\frac{\Delta\eta(y)}{\Delta x(y)}, \tag{1}$$

where $\Delta\,x(y)$ represents the latitudinally varying width of the basin, g is the Earth gravitational constant and f is the Coriolis parameter. Resulting velocity anomalies (Figure 8c) are always negative, i.e., directed toward the equator, and vary on a variety of timescales, including the seasonal cycle. They reach a maximum after 3–4 years in the subpolar North Atlantic and after about 7 years in midlatitudes.

[39] Because the model is closed at its northern boundary, the near-surface southward velocities shown in Figure 8c have to be compensated at depths, implying that the MOC has to slow down. This is illustrated in Figure 9, showing the global MOC anomalies resulting from Greenland freshwater forcing after 7 years. The figure suggests a 1 Sv reduction of the MOC at about 50°N. Negative anomalies reach from 60°N to 60°S; however, clearly enhanced negative amplitudes reside in the northern hemisphere.

[40] To further investigate the timescales involved in this adjustment of the MOC during the 50-year run, we show in Figure 9b time series of the maximum changes in the Atlantic MOC as function of latitude. While the early slowdown of the MOC can be seen around 60°N, i.e., close to the freshwater source, the extension of this negative anomaly quickly spreads southward, reaching 45°S after only 5–6 years, equivalent to a phase speed of about 8 cm/s. However, the spreading is faster north of the equator, and slows down subsequently. Some slowdown can also be observed during the transition from the subpolar to the subtropical gyre around 45°N (i.e., near Flemish Cap). Figure 9b suggests that, owing to enhanced freshwater forcing around Greenland, the ocean circulation adjusts rather quickly in its MOC component in high latitudes, where MOC amplitudes reduce by about 1.5 Sv within the first 2 years, without any further drift obvious subsequently. The adjustment of much of the remaining part of the North Atlantic takes substantially longer and at the end of the 50-year run has not yet reached a new equilibrium, especially in the southern hemisphere, consistent with continuing adjustments of the density field.

[41] Associated with the slowdown of the MOC is a reduction in the meridional heat transport in the Atlantic Ocean (Figure 9c). But in contrast to the MOC anomaly pattern that is maximum in the subpolar North Atlantic, a significant heat transport reduction can be found between 15°N and 45°N, i.e., in the subtropical gyre. Superimposed to the large-scale adjustments in MOC strengths and the meridional heat transport in the Atlantic, pronounced quasi-decadal oscillation in both variables can be observed. These oscillations were already visible in time series of the Atlantic heat content (Figure 5), of SSH anomalies (Figure 7) and in the basin-averaged meridional surface velocities (Figure 8c). We can see now from Figure 9, that an associated anomaly in MOC and heat transport appears first in year 8 and later in the years 17, 25, and 39. During all those instances, a clear increase in SSH can be observed in the North Atlantic (compare to Figure 7).

[42] The oscillations visible in Figure 9 are quite similar in character to results published by *Eden and Willebrand* [2001, their Figure 6]. The authors studied the variability of the Atlantic circulation using a numerical model and found that many transport characteristics showed variability on a quasi-decadal period, including that of the MOC. This variability was studied subsequently in more detail by *Eden and Jung* [2001] who showed that the observed/modeled developments of interdecadal SST anomalies can be traced back to the lagged response (10–20 years) of the North Atlantic thermohaline circulation and the subpolar gyre strength to interdecadal variability in the surface net heat flux forcing, in their case associated with the NAO. We seem to see here a similar quasi-decadal oscillation, but entirely triggered by internal model dynamics and associated feedbacks to the atmosphere.

4. Response From Antarctica

[43] *Bryan* [1996] suggested in his simple reduced-gravity model that the regional and global response to density perturbations around Antarctica are quite distinct and much smaller than those occurring in the North Atlantic. Similarly, *Johnson and Marshall* [2004] showed that the impact of density anomalies on the circulation of the Atlantic exhibits a clear asymmetry in that perturbations from the southern hemisphere do not affect the North Atlantic meridional overturning circulation (MOC) in a clear way on short timescales.

[44] To investigate whether this is a general result that applies also to enhanced freshwater forcing through ice melting, we performed a second experiment in which the surface freshwater forcing was perturbed by the pattern shown in Figure 1b. Associated changes in SSH (Figure 10), confirm that SSH anomalies, originating from Antarctica, to first order, stay south of the ACC region and only slowly spread over larger areas in the southern hemisphere. Accordingly, basin averaged SSH anomalies increase much slower than what can be found from the Greenland experiment (Figure 7b). The largest increase can now be found in the South Atlantic sector reflecting

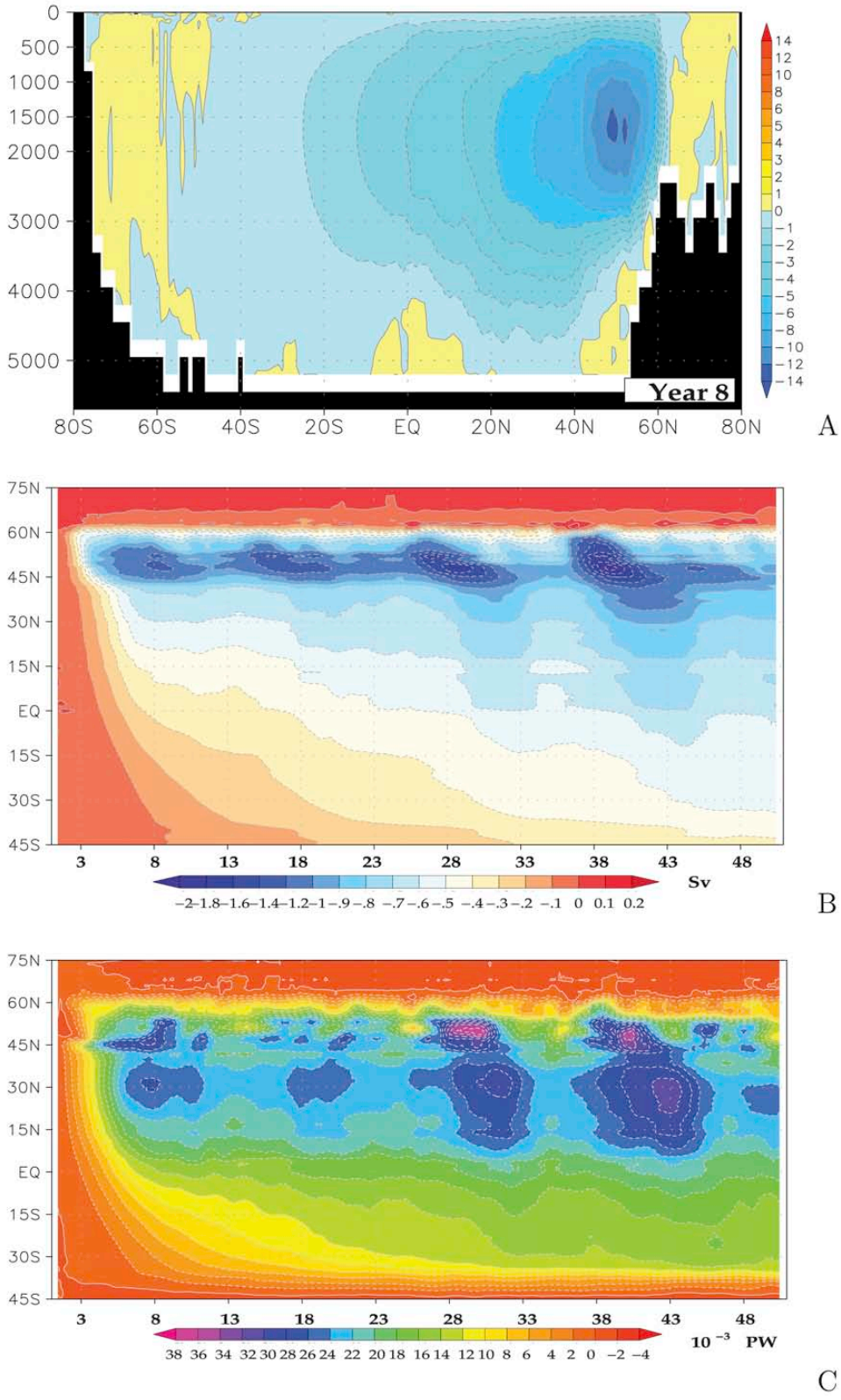

Figure 9. (a) Annual mean of the anomaly of the MOC during year 7 of the perturbed run. A negative anomaly indicates a reduction of the background state. (b) Time-latitude plot of the maximum of the MOC anomaly as it appears at each latitude. (c) Time-latitude plot of meridional heat transport anomalies. In Figures 9b and 9c the numbers on the *x* axis denote model years.

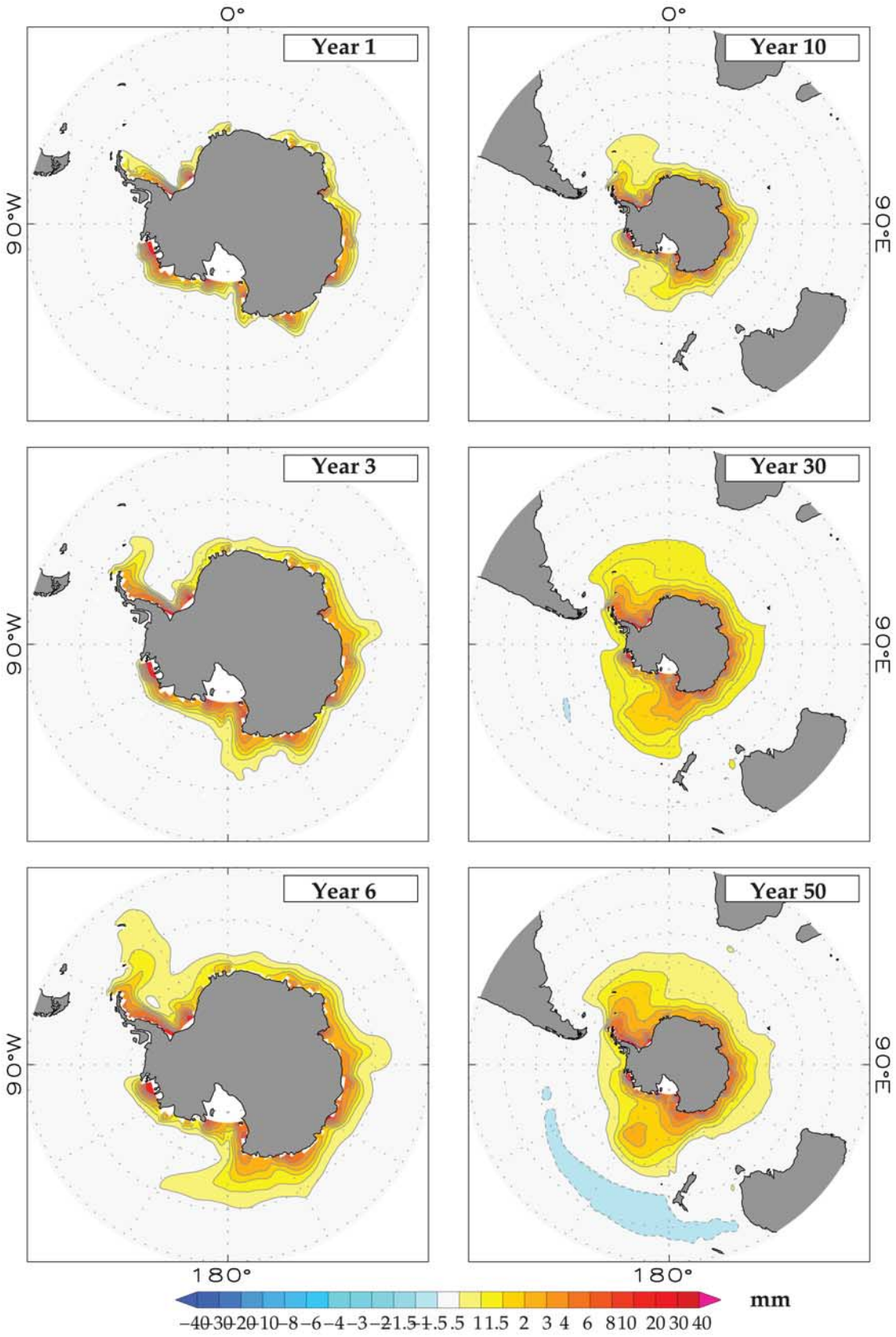

Figure 10. December-mean anomalies of SSH resulting from a freshwater source around Antarctica (compare Figure 1b). (left) SSH anomalies around the Antarctic continent from the years 1, 3, and 6. (right) Similar fields, but for the years 10, 30, and 50 of the perturbed run.

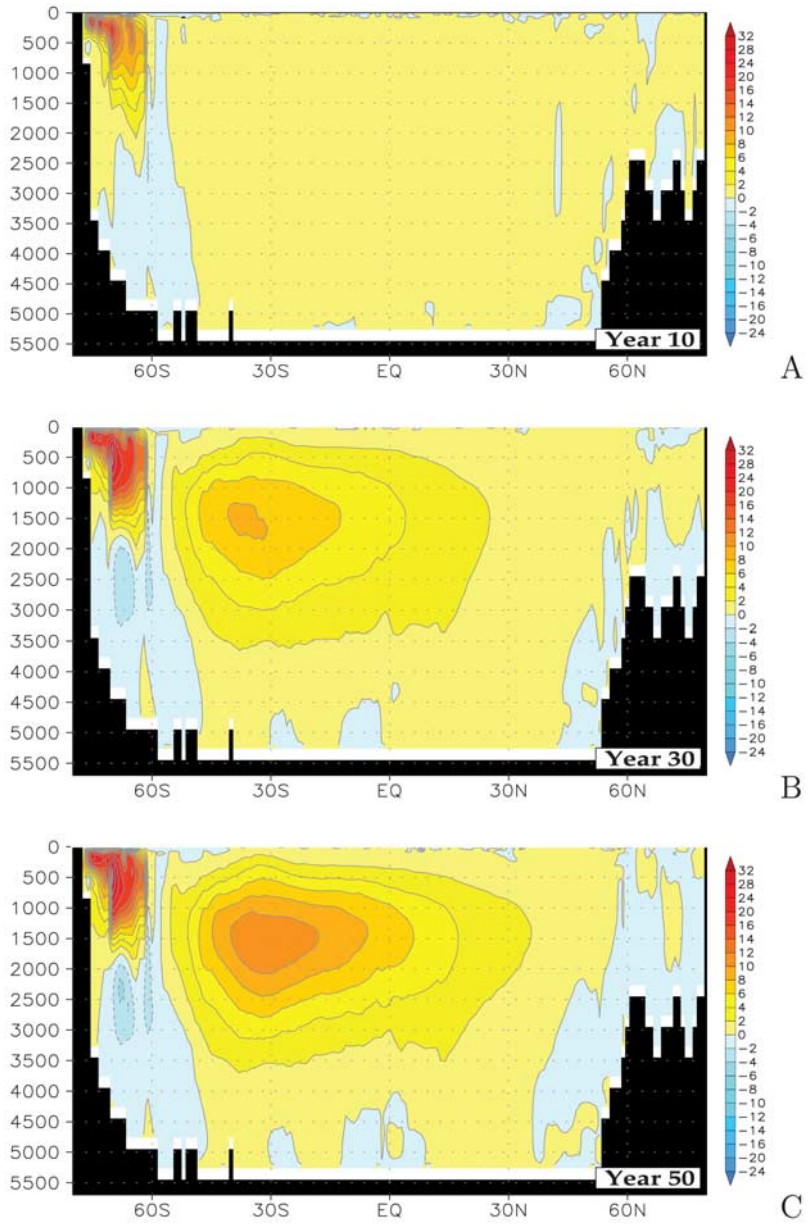

Figure 11. Annual mean of the anomaly of the MOC during (a) year 10, (b) year 30, and (c) year 50. A positive anomaly indicates an enhancement of the background state.

the SSH increase over of the Weddell Sea. The SSH increase is smaller in all other basins of the southern hemisphere and is barely measurable in the North Atlantic and North Pacific. Moreover, it is apparent that the SSH adjustment timescale is much longer in all basins as compared to the response to Greenland forcing.

[45] We note that the response of the ocean circulation to Antarctic freshwater forcing remains localized also in terms of MOC over the first few decades (Figure 11). Only after 30 years, some reaction becomes visible at mid depth in the southern hemisphere, and the MOC anomaly, does not spread northward across the equator before the end of the run. We note also the marked difference to the response to Greenland melting in that now the MOC is strengthened, especially in the southern hemisphere, while in the previous case the MOC was reduced over most of the Atlantic Ocean. This finding is consistent with results from *Stouffer et al.* [2006] who investigated the response of an atmosphere-ocean coupled general circulation model (AOGCM) to perturbations of freshwater fluxes across the sea surface in the North Atlantic and Southern Ocean. However, because their freshening with 1 Sv freshwater input was stronger, results are not comparable, quantitatively, with ours.

5. Concluding Remarks

[46] In this paper we investigated the transient response of the ocean circulation to freshwater forcing associated

with enhanced melting of the Greenland and Antarctic ice sheets. Our results confirm earlier studies suggesting that the global ocean is less sensitive to perturbations in surface buoyancy fluxes imposed to the southern ocean than those acting over the North Atlantic. Although previous studies [e.g., *Bryan*, 1996; *Hsieh and Bryan*, 1996; *Huang et al.*, 2000] were primarily concerned with heat content anomalies due to an atmospheric CO_2 increase, our results confirm that those results to some extent also hold in the context of anomalous freshwater forcing associated with enhanced melting of polar ice caps. If this melting continues at the current pace [*Velicogna and Wahr*, 2005; *Rignot and Kanagaratnam*, 2006], or even accelerates over the next decade, we should expect a measurable reaction of the ocean circulation and of regional and basin-wide SSH to this large amount of extra freshwater added from Greenland to the North Atlantic.

[47] Timescales for a first response of the Atlantic are just a few years in the subpolar North Atlantic and 5–10 years for the Atlantic and global ocean. However, at the end of our 50-year run, no equilibrium was reached in any basin. The corollary of our findings is that melt water dumped into the North Atlantic from Greenland will reside first of all in the Atlantic and will only slowly propagate into the other basins. In particular, it will take a significant length of time until the Pacific Ocean will "feel" this extra volume, for example, in form of sea level rise. This is an important result since it implies that melting of Greenland's ice cap is much less of a threat to tropical islands in the Pacific than it is for the coasts of North America and Europe.

[48] In agreement with *Bryan* [1996], *Hsieh and Bryan* [1996], and *Huang et al.* [2000] on the basis of simple reduced-gravity dynamics, from primitive equation dynamics we find here again a general response pattern to freshwater forcing that establishes a basin wide and global adjustment to in form of Kelvin/Rossby waves. However, advective processes and air-sea interaction appear to be important elements of the long-term adjustment as well. In particular, changes in the oceans heat content due to modified air-sea interactions modify SSH of the central basin and the feedback with the circulation then leads to a reduced MOC strength and associated positive southward heat transport anomalies in the North Atlantic, which in turn cause SSH to increase in low latitudes and in the southern hemisphere as discussed previously by *Bryan* [1996].

[49] An important question is whether a given pattern in sea level change, such as revealed here in response to Greenland ice melting, can be used as a "finger print" of enhanced Greenland ice melting. Essentially, such a fingerprint concept requires a detailed knowledge of natural SSH variability and those induced by changes in surface heat fluxes and wind stress, so that one can discriminate the latter effects from changes originating from ice melting. Our results suggest that the largest SSH increase in response to Greenland ice melting should be observable along the coastal Atlantic, notably the west coast, which is even further increased through the negative depression of up to 5 cm occurring in the central basin. However, in a recent study *Mitrovica et al.* [2001] suggest that because melting of ice sheets will reduce the height of the geoid in their vicinity, it consequently will also lower sea level around the regions of ice melting of polar ice sheets [see also *Tamisea et al.*, 2001]. The authors suggest the resulting pattern of sea level reduction should be detectable in measurements of decreasing SSH, especially along continental coasts. However, because of the strong dynamic increase of SSH to freshwater forcing discussed here, it appears more likely to detect the dynamic response in sea level presented here using satellite altimeter data, partly because preliminary discussions suggest that the gravity impact on sea level is smaller than the dynamic response (R. Ray, personal communication, 2007).

[50] Further research is required to thoroughly analyze all causes of observed SSH changes in the North Atlantic before pattern similar to those suggested here resulting from Greenland ice melting can be detected and before a gravity response can be separated from a dynamical response. Along those lines, *Lombard et al.* [2005] show the difference T/P–Ishii thermosteric sea level trend for the period 1993–1998. Their results show intriguing similarities to the pattern of SSH change shown here in response to Greenland freshwater forcing. However, a comparison is not straight forward, because our results represent a mixture of freshwater-induced changes and of thermosteric changes associated with modified air-sea interactions. This suggests that the oceans adjustment to anomalous freshwater forcing from melting polar ice caps is a coupled ocean-atmosphere problem and needs to be studied using a fully coupled model, similar to what was started by *Stouffer et al.* [2006]. The future will need to see more studies that also investigate the joint effect of melting of Greenland and Antarctica on regional and global sea level and on the circulation. Results will provide an understanding and thereby a better basis for separating the effect of dynamics and kinematics from gravity induced SSH changes in coastal and regional observations of sea level.

[51] **Acknowledgments.** Kyozo Ueyoshi helped with all aspects of the computations. The idea for this study goes back to early discussions with Carl Wunsch and Walter Munk. We appreciate the extensive comments of anonymous referees who helped significantly to improve the manuscript. The computational support from the National Center for Atmospheric Research and the Scripps COMPAS computing facility is acknowledged. Support was provided in part through a grant from the Melon Foundation, through a NASA grant (NAG5-8623), and through ONR (NOPP) grant N00014-99-1-1049. Support was also provided in part through grant NA17RJ1231 (NOAA) "SIO Participation in US GODAE." This is a contribution of the Consortium for Estimating the Circulation and Climate of the Ocean (ECCO) funded by the National Oceanographic Partnership Program.

References

Arakawa, A., and V. R. Lamb (1977), Computational design of the basic dynamical processes of the UCLA general circulation model, in *General Circulation Models of the Atmosphere*, *Methods Comput. Phys.*, vol. 17, edited by J. Chang, pp. 174–265, Academic Press, San Diego, Calif.

Broecker, W. S., et al. (1989), Routing of melt water from the Laurentine ice-sheet during the Younger Dryas cold episode, *Nature*, *341*, 318–321.

Bryan, K. (1996), The steric component of sea level rise associated with enhanced greenhouse warming: A model study, *Clim. Dyn.*, *12*, 545–555.

Cessi, P., and P. Otheguy (2003), Oceanic tele-connections: Remote response to decadal wind forcing, *J. Phys. Oceanogr.*, *33*, 1604–1617.

Cessi, P., K. Bryan, and R. Zhang (2004), Global seiching of the thermocline waters without volume change between the Atlantic and the Indian-Pacific Ocean Basins, *Geophys. Res. Lett.*, *31*, L04302, doi:10.1029/2003GL019091.

Church, J. A., J. M. Gregory, P. Huybrechts, M. Kuhn, K. Lambeck, M. T. Nhuan, D. Qin, and P. L. Woodworth (2001), Changes in sea level, in *Climate Change 2001: The Scientific Basis. Contribution of Working*

Group I to the Third Assessment Report of the Intergovernmental Panel on Climate Change, edited by J. T. Houghton et al., pp. 639–693, Cambridge Univ. Press, Cambridge, U.K.

Dyurgerov, M. B., and M. F. Meier (2005), Glaciers and the changing Earth system: A 2004 snapshot, *Occas. Pap. 58*, 117 pp., Inst. of Arct. and Alp. Res., Univ. of Colo., Boulder.

Eden, C., and T. Jung (2001), North Atlantic interdecadal variability: Oceanic response to the North Atlantic Oscillation (1865–1997), *J. Clim.*, *14*, 676–691.

Eden, C., and J. Willebrand (2001), Mechanism of interannual to decadal variability of the North Atlantic circulation, *J. Clim.*, *14*, 2266–2280.

Garnier, E., B. Barnier, L. Siefridt, and K. Béranger (2000), Investigating the 15 years air-sea flux climatology from the ECMWF re-analysis project as a surface boundary condition for ocean models, *Int. J. Climatol.*, *20*, 1653–1673.

Gent, P. R., and J. C. McWilliams (1990), Isopycnal mixing in ocean models, *J. Phys. Oceanogr.*, *20*, 150–155.

Gerdes, R., W. Hurlin, and S. M. Griffies (2006), Sensitivity of a global ocean model to increased run-off from Greenland, *Ocean Modell.*, *12*, 416–435.

Goodman, P. J. (2001), Thermohaline adjustment and advection in an OGCM, *J. Phys. Oceanogr.*, *31*, 1477–1497.

Greatbatch, R. J. (1994), A note on the representation of steric sea-level in models that conserve volume rather than mass, *J. Geophys. Res.*, *99*, 12,767–12,771.

Hsieh, W., and K. Bryan (1996), Redistribution of sea level rise associated with enhanced greenhouse warming: A simple model study, *Clim. Dyn.*, *12*, 759–762.

Hsieh, W. M., M. K. Davey, and R. C. Wajsowicz (1983), The free Kelvin wave in finite-difference numerical models, *J. Phys. Oceanogr.*, *13*, 1383–1397.

Huang, R., M. Cane, N. Naik, and P. Goodman (2000), Global adjustment of the thermocline in response to deep-water formation, *Geophys. Res. Lett.*, *27*, 759–762.

Jacobs, S. S., H. H. Hellmer, C. S. M. Doake, A. Jenkins, and R. M. Frolich (1992), Melting of ice shelves and the mass balance of Antarctica, *J. Glaciol.*, *38*, 375–387.

Jacobs, S. S., H. H. Hellmer, and A. Jenkins (1996), Antarctic ice sheet melting in the South Pacific, *Geophys. Res. Lett.*, *23*, 957–960.

Johnson, H. L., and D. P. Marshall (2004), Global teleconnections of meridional overturning circulation anomalies, *J. Phys. Oceanogr.*, *34*, 1702–1722.

Kalnay, E., et al. (1996), The NCEP/NCAR re-analysis project, *Bull. Am. Meteorol. Soc.*, *77*, 437–471.

Köhl, A., D. Stammer, and B. Cornuelle (2007), Variability of the meridional overturning in the North Atlantic from the 50 years GECCO state estimation, *J. Phys. Oceanogr.*, *37*, 313–337.

Krabill, W., et al. (2004), Greenland Ice Sheet: Increased coastal thinning, *Geophys. Res. Lett.*, *31*, L24402, doi:10.1029/2004GL021533.

Landerer, F., J. Jungclaus, and J. Marotzke (2007), Dynamic and steric sea level change in response to the A1B-IPCC scenario, *J. Phys. Oceanogr.*, *37*, 296–312.

Large, W. G., J. C. McWilliams, and S. C. Doney (1994), Oceanic vertical mixing: A review and a model with nonlocal boundary layer parameterization, *Rev. Geophys.*, *32*, 363–403.

Levitus, S., M. E. Conkright, T. P. Boyer, T. O. Brien, J. Antonov, C. Stephens, L. Stathoplos, D. Johnson, and R. Gelfeld (1998), *World Ocean Database 1998, vol. 1, Introduction, NOAA Atlas NESDIS 18*, 346 pp., NOAA, Silver Spring, Md.

Lombard, A., et al. (2005), Contribution of thermal expansion to present-day sea-level change revisited, *Global Planet. Change*, *47*, 1–16.

Marshall, J., A. Adcroft, C. Hill, L. Perelman, and C. Heisey (1997a), A finite-volume, incompressible Navier-stokes model for studies of the ocean on parallel computers, *J. Geophys. Res.*, *102*, 5753–5766.

Marshall, J., C. Hill, L. Perelman, and A. Adcroft (1997b), Hydrostatic, quasi-hydrostatic and non-hydrostatic ocean modeling, *J. Geophys. Res.*, *102*, 5733–5752.

Mitrovica, J. X., M. E. Tamisea, J. L. Davis, and G. A. Milne (2001), Recent mass balance of polar ice sheets inferred from pattern of global sea level change, *Nature*, *409*, 1026–1029.

Nerem, R. S., E. Leuliette, and A. Cazenave (2006), Present-day sea-level change: A review, *C. R. Geosci.*, *338*(14–15), 1077–1083.

Prange, M., and R. Gerdes (2005), The role of surface freshwater flux boundary conditions in Arctic Ocean modeling, *Ocean Modell*, *13*, 25–43.

Reynolds, R. W., N. A. Rayner, T. M. Smith, D. C. Stokes, and W. Wang (2002), An improved in situ and satellite SST analysis for climate, *J. Clim.*, *15*, 1609–1625.

Rignot, E., and F. Kanagaratnam (2006), Changes in the velocity structure of the Greenland ice sheet, *Science*, *311*(5763), 986–990.

Smith, W. H. F., and D. T. Sandwell (1997), Global seafloor topography from satellite altimetry and ship depth soundings, *Science*, *277*, 195–196.

Stammer, D., C. Wunsch, I. Fukumori, and J. Marshall (2002), State estimation improves prospects for ocean research, *Eos Trans. AGU*, *83*(27), 289, 294–295.

Stammer, D., K. Ueyoshi, A. Köhl, W. B. Large, S. Josey, and C. Wunsch (2004), Estimating air-sea flux estimates through global ocean data assimilation, *J. Geophys. Res.*, *109*, C05023, doi:10.1029/2003JC002082.

Stouffer, R. J., D. Seidov, and B. J. Haupt (2006), Climate response to external sources of freshwater: North Atlantic versus the Southern Ocean, *J. Cim.*, *20*, 436–448.

Tamisea, M. E., J. X. Mitrovica, G. A. Milne, and J. L. Davis (2001), Global geoid and sea level change due to present-day ice mass fluctuations, *J. Geophys. Res.*, *106*, 30,849–30,863.

Thomasi, R., E. Frederick, W. Krabill, S. Manizade, and C. Martin (2006), Progressive increase in ice loss from Greenland, *Geophys. Res. Lett.*, *33*, L10503, doi:10.1029/2006GL026075.

Velicogna, I., and J. Wahr (2005), Greenland mass balance from GRACE, *Geophys. Res. Lett.*, *32*, L18505, doi:10.1029/2005GL023955.

Wunsch, C., and P. Heimbach (2006), Estimated decadal changes in the North Atlantic meridional overturning circulation and heat flux 1993–2004, *J. Phys. Oceanogr.*, *36*, 2012–2024.

Wunsch, C., R. Ponte, and P. Heimbach (2007), Decadal trends in sea level pattern: 1993–2004, *J. Clim.*, *20*, 5889–5911.

Zwally, H. J., M. B. Giovinetto, J. Li, H. G. Cornejo, M. A. Beckly, A. C. Brenner, J. L. Saba, and D. Yi (2005), Mass changes of the Greenland and Antarctic ice sheets and shelves and contributions to sea level rise: 1992–2002, *J. Glaciol.*, *51*, 509–527.

D. Stammer, Institut für Meereskunde, Universität Hamburg, Bundestrasse 53, D-20146 Hamburg, Germany. (stammer@ifm.uni-hamburg.de)